The Heterolytic Dissociation of Neutral and Protonated Nitrous Acid

Hong Wu and Rainer Glaser*

Department of Chemistry, University of Missouri-Columbia, Columbia, Missouri 65211

Received: April 28, 2003; In Final Form: September 30, 2003

Structures, energies, and vibrational properties of HONO and H_2ONO^+ and of their dissociation products NO^+, HO^-, and water were studied with the DFT methods B3LYP and MPW1PW91 and with the configurational methods MP2, QCISD, QCISD(T), CCSD, and CCSD(T) in conjunction with the basis sets 6-31G**, 6-31++G**, 6-311G**, 6-311++G**, 6-311++G(2d,p), and 6-311++G(2df,2p). The multilevel methods G1, G2, G2(MP2), G3, and CBS-Q also were employed. The experimental trans-preference energy $\Delta E_0^{Pref} = 1.555 \pm 0.167$ kJ/mol of HONO is reproduced well at all levels with good basis sets. On the basis of the CCSD(T)/6-311++G(2df,2p) energies and the thermochemical data, our best computed estimate is $\Delta E_0^{Pref} = 1.83$ kJ/mol. The experimental heterolytic bond dissociation energy of $\Delta E_0 = 917.80$ kJ/mol for HONO and of $\Delta H_{298} = 77.3$ kJ/mol for H_2ONO^+ are more difficult to reproduce. At the CCSD(T)/6-311++G(2df,2p) level, we found $\Delta E_0 = 925.5$ kJ/mol and $\Delta H_{298} = 81.6$ kJ/mol. The MP2, QCISD, and CCSD methods yield reasonable results when used with larger basis sets. The G2 method as well as the G2-mimics G2(MP2) and G3 also yield reasonable results. The density functional methods performed significantly worse than the MP2(full), QCISD, and CCSD methods. The structures of *E*- and *Z*-HONO, of the electrostatic complex H_2ONO^+, and of the dissociation products also are discussed. Effects of aqueous solvation were examined with the IPCM method at DFT, MP2, and QCISD levels with the 6-311++G(2df,2p) basis set. Only the proton-catalyzed heterolysis plays a role at ambient temperatures, and our results suggests different mechanisms for NO^+ formation in gas-phase and in solution.

Introduction

Nitrous acid, HONO, plays an important role in atmospheric chemistry[1] and is an essential intermediate in combustions.[2] Nitrous acid is a well-known source of the nitrosonium ion NO^+ in organic synthetic chemistry.[3] The significance of HONO in toxicology has also been well established[4] and, in particular, includes the nitrosation chemistry of amines.[5] We are currently studying the chemistry of α-hydroxynitrosamines because of their putative role in the carcinogenesis of nitrosamines.[6] In this context, we are interested in the intrinsic energetics of the addition of HONO to imines. The discussion of the stepwise addition requires the knowledge of the heterolytic dissociation energy of HONO.

$$HO-N=O \rightarrow H-O^- + {}^+N=O$$

The heterolytic dissociation energy of nitrous acid has never been reported—neither in solution nor in the gas phase. The accurate computation of the heterolysis of HONO is not trivial. In their CCSD(T) study of the trans-preference energy, Lee and Rendell pointed out that nondynamical electron correlation is important for nitrous acid.[7] The cation NO^+ is isoelectronic with carbon monoxide and the great difficulty of adequately describing its electronic structure is well-known. In the present paper, we derive an experimental dissociation energy of nitrous acid based on the homolytic dissociation energy of nitrous acid, the electron affinity of OH, and the ionization energy of NO. This experimental value is then employed to calibrate the computed heterolytic dissociation energies. Comparison is made to the proton-catalyzed heterolysis reaction. The nitrous acidium ion H_2ONO^+ easily dissociates into water and NO^+. We report the proton affinity of HONO and the heterolysis of H_2ONO^+ and compare both of these values to the respective experimental data. In addition, we report approximate effects of solvation of the relative isomer stabilities, the heterolyses of HONO and H_2ONO^+, and the proton affinity of HONO.

$$HO-N=O + H^+ \rightarrow H_2O\text{---}{}^+N=O$$

$$H_2O\text{---}{}^+N=O \rightarrow H_2O + {}^+N=O$$

Calibration is a key feature of all the model theories that are widely used in chemistry. The calibration involves a well-defined set of molecular properties and reactions. Whenever a property is considered for a molecule that is not represented by the set, then one needs to establish the performance of the methods performed for this problem by comparison to experimental data. Aside from our specific interest, our work should have a broader impact as it informs about the performance of a variety of widely used methods in related systems and applications.

Computational Methods

The structures were fully optimized using four theoretical approaches: density functional theory,[8] second-order Møller−Plesset perturbation theory MP2,[9] quadratic configuration interaction theory with single and double excitations QCISD,[10] and coupled cluster theory using single and double substitutions CCSD.[11] Restricted calculations were performed at all levels and for all molecules. Triple excitations were considered additionally at the levels QCISD(T) and CCSD(T).[10] Among the density functional methods, we chose the hybrid density functional methods B3LYP and MPW1PW91. Hybrid methods

* Corresponding author. E-mail: GlaserR@missouri.edu.

10.1021/jp035149m CCC: $25.00
Published on Web 11/15/2003

TABLE 1: Structures of Nitrous Acid, Protonated Nitrous Acid, and Their Dissociation Products[a]

		HONO and H_2ONO^+						dissociation fragments			
method & basis set	molecule	HO	O−N	N═O	HOH	HON	ONO	NO	HO	HO	HOH
B3LYP/6-311++G(2df,2p)	*E*-HONO	0.968	1.429	1.164		102.9	111.0	1.057	0.965		
	Z-HONO	0.978	1.389	1.177		106.4	113.9				
	H_2ONO^+	0.970	2.173	1.073	106.0	113.4	104.5			0.961	105.2
MPW1PW91/6-311++G(2df,2p)	*E*-HONO	0.964	1.398	1.162		103.2	111.3	1.053	0.961		
	Z-HONO	0.975	1.365	1.174		106.4	113.9				
	H_2ONO^+	0.966	2.122	1.067	106.0	113.4	104.6			0.957	105.0
MP2(full)/6-311++G(2df,2p)	*E*-HONO	0.967	1.415	1.176		101.9	111.0	1.079	0.963		
	Z-HONO	0.977	1.379	1.189		104.9	113.5				
	H_2ONO^+	0.963	2.278	1.083	104.9	122.5	98.5			0.958	104.3
QCISD(full)/6-311++G(2df,2p)	*E*-HONO	0.962	1.405	1.167		102.8	111.0	1.061	0.961		
	Z-HONO	0.971	1.375	1.179		105.4	113.5				
	H_2ONO^+	0.960	2.317	1.064	104.9	124.2	98.4			0.956	104.6
QCISD(fc,T)/6-311++G(2df,2p)	*E*-HONO	0.966	1.428	1.172		102.1	110.8	1.068	0.963		
	Z-HONO	0.975	1.392	1.185		104.8	113.4				
	H_2ONO^+	0.963	2.271	1.072	104.9	122.6	99.4			0.958	104.3
CCSD(fc)/6-311++G(2df,2p)	*E*-HONO	0.963	1.401	1.167		102.9	110.9	1.060	0.961		
	Z-HONO	0.972	1.373	1.178		105.5	113.5				
	H_2ONO^+	0.961	2.324	1.062	104.9	124.5	98.3			0.957	104.5
CCSD(fc,T)/6-311++G(2df,2p)	*E*-HONO	0.967	1.425	1.174		102.1	110.8	1.068	0.964		
	Z-HONO	0.976	1.390	1.186		104.8	113.4				
	H_2ONO^+	0.964	2.277	1.072	104.8	122.8	99.3			0.959	104.3
MP2(full)/6-31G(d)[b]	*E*-HONO	0.980	1.423	1.197		101.9	110.3	1.103	0.980		
	Z-HONO	0.991	1.385	1.209		104.5	112.8				
	H_2ONO^+	0.977	2.193	1.109	104.8	119.4	100.3			0.969	104.0
MP2(full)/6-31G(d′)[c]	*E*-HONO	0.972	1.416	1.185		102.8	110.7	1.090	0.979		
	Z-HONO	0.984	1.376	1.198		106.0	113.2				
	H_2ONO^+ (np)	0.968	2.203	1.094	106.6	121.8	99.8			0.962	105.9
	H_2ONO^+ (p)	0.967	2.160	1.094	107.5	135.1/117.4	107.8				

[a] Distances in angstroms and angles in degrees. [b] Optimized geometry employed at G1, G2, and G3. [c] Optimized geometry employed in CBS-Q level.

combine the Hartree−Fock exchange with exchange-correlation density functionals. The B3LYP method combines the Slater exchange functional along with corrective terms for the density gradient developed by Becke[12] with the correlation functional by Lee, Yang, and Parr.[13] The B3LYP method has become widely used and it is considered highly accurate.[14,15] The MPW1PW91 method involves Barone's modified Perdew-Wang 1991 exchange functional[16] in combination with the 1991 gradient-corrected correlation functional by Perdew and Wang.[17,18]

We employed the following six basis sets: 6-31G**, 6-31++G**, 6-311G**, 6-311++G**, 6-311++G(2d,p) and 6-311++G(2df,2p).[19,20,21,22] Each basis set was employed in conjunction with each theoretical method. The CCSD and the computations with triple excitations were carried out only with the largest basis set 6-311++G(2df,2p). All structures were optimized at 27 theoretical levels and pertinent structures and energies are reported in Tables 1 and 2, respectively.

The Pople basis sets are widely used in the organic chemistry community because these basis sets succeed so well in reproducing experimental data with high accuracy. Their performance has been well established over many years by careful calibration studies. The basis sets emphasize the description of valence electron density and in doing so it is assumed that core density remains largely unchanged. In some correlation calculations all orbitals were correlated (full) while others employed the frozen-core (fc) approximation. The calculations in which all orbitals are correlated are not meant to suggest that they would account well for core electron correlation since the basis sets do not include functions to correlate the core.

To obtain thermodynamic corrections, vibrational analyses were carried out at each level using the best basis set. The results are summarized in a table in the Supporting Information where we report the molecular vibrational zero-point energy (*ZPE*), the internal thermal energy due to translation, rotation, and vibration ($TE = E_t + E_r + E_v$), and the entropy (*S*). We use these data to compute the energy at absolute zero, $E_0 = E + ZPE$, and 298 K, $E_{298} = E + TE$, the enthalpy at 298 K, $H_{298} = E_{298} + RT$, and the Gibbs free enthalpy at 298 K, $G_{298} =$

TABLE 2: Isomer Preference Energies and Dissociation Energies[a]

	HONO		H_2ONO^+
method & basis set	ΔE^{pref}	ΔE^{diss}	ΔE^{diss}
B3LYP			
6-31G**	−3.76	1168.92	146.45
6-31++G**	1.75	994.46	122.52
6-311G**	−0.99	1121.31	136.72
6-311++G**	4.51	974.98	117.43
6-311++G(2d,p)	2.31	976.42	114.62
6-311++G(2df,2p)	2.74	976.61	112.09
MPW1PW91			
6-31G**	−4.54	1172.13	140.46
6-31++G**	0.57	1010.48	119.62
6-311G**	−1.87	1125.91	131.45
6-311++G**	3.14	990.95	114.63
6-311++G(2d,p)	0.95	992.87	111.72
6-311++G(2df,2p)	1.31	993.83	109.35
MP2(full)			
6-31G**	−4.74	1074.26	104.97
6-31++G**	1.73	903.94	93.91
6-311G**	−1.83	1039.50	99.03
6-311++G**	4.53	890.31	89.97
6-311++G(2d,p)	2.32	898.72	89.57
6-311++G(2df,2p)	1.73	914.04	87.18
QCISD(full)			
6-31G**	−3.92	1086.76	101.28
6-31++G**	1.76	928.22	91.52
6-311G**	−1.31	1051.18	95.75
6-311++G**	4.41	914.14	87.83
6-311++G(2d,p)	2.19	918.72	86.61
6-311++G(2df,2p)	1.72	935.27	84.54
QCISD(fc,T)			
6-311++G(2df,2p)	2.06	944.38	86.90
CCSD(fc)			
6-311++G(2df,2p)	1.62	934.13	83.85
CCSD(fc,T)			
6-311++G(2df,2p)	1.83	941.89	86.41

[a] Relative energies in kJ/mol.

TABLE 3: Thermodynamical Values[a,b]

	methods	ΔE	ΔE_0	ΔE_{298}	ΔH_{298}	ΔG_{298}
trans-preference energy	B3LYP	2.74	2.57	2.37	2.37	2.62
	MPW1PW91	1.31	1.08	0.94	0.94	1.13
	MP2(full)	1.73	1.94	1.73	1.73	2.01
	QCISD(full)	1.72	1.76	1.55	1.55	1.78
	QCISD(fc,T)	2.06	2.06	1.85	1.85	2.11
	CCSD(fc)	1.62	1.61	1.44	1.44	1.64
	CCSD(fc,T)	1.83	1.83	1.63	1.63	1.88
	G1		3.37	3.17	3.17	3.40
	G2		2.53	2.32	2.32	2.55
	G2(MP2)		2.27	2.07	2.07	2.29
	G3		2.62	2.41	2.41	2.63
	CBS-Q		2.38	2.19	2.19	2.39
heterolysis of neutral nitrous acid	B3LYP	976.61	960.89	964.78	967.26	930.91
	MPW1PW91	993.83	977.23	981.24	983.72	947.13
	MP2(full)	914.04	897.19	901.08	903.56	867.07
	QCISD(full)	935.27	918.42	922.16	924.64	888.11
	QCISD(fc,T)	944.38	928.08	931.93	934.41	898.05
	CCSD(fc)	934.13	916.97	920.97	923.45	886.89
	CCSD(fc,T)	941.89	925.47	929.37	931.84	895.46
	G1		922.82	926.83	929.31	892.63
	G2		918.39	922.40	924.88	888.19
	G2(MP2)		917.02	921.03	923.51	886.83
	G3		925.75	929.76	932.24	895.56
	CBS-Q		930.76	934.85	937.33	900.54
heterolysis of protonated nitrous acid	B3LYP	112.09	104.03	104.84	107.32	78.16
	MPW1PW91	109.35	101.44	104.50	106.98	69.21
	MP2(full)	87.18	80.02	79.96	82.44	51.61
	QCISD(full)	84.54	77.46	77.20	79.68	51.53
	QCISD(fc,T)	86.90	79.74	79.64	82.12	53.30
	CCSD(fc)	83.85	76.81	76.49	78.97	50.93
	CCSD(fc,T)	86.41	79.23	79.12	81.60	52.85
	G1		84.64	83.86	86.34	64.19
	G2		79.65	78.87	81.35	59.20
	G2(MP2)		78.65	77.87	80.35	58.22
	G3		80.49	79.83	82.31	57.28
	CBS-Q (H_2ONO^+ (p))		79.64	81.71	84.19	50.57
	(H_2ONO^+ (p))		79.45	79.59	82.07	53.02
proton affinity of nitrous acid	B3LYP	795.40	769.50	768.88	771.36	751.20
	MPW1PW91	791.88	766.56	768.07	770.55	743.75
	MP2(full)	832.89	808.64	807.16	809.64	789.67
	QCISD(full)	829.37	804.96	803.20	805.68	786.70
	QCISD(fc,T)	818.05	792.97	791.48	793.96	774.14
	CCSD(fc)	830.89	806.62	804.78	807.26	788.42
	CCSD(fc,T)	819.97	795.05	793.51	795.99	776.27
	G1		783.71	781.39	783.87	770.96
	G2		785.62	783.30	785.78	772.87
	G2(MP2)		787.98	785.66	788.14	775.23
	G3		785.71	783.51	785.99	770.20
	CBS-Q (H_2ONO^+ (p))		781.06	781.50	783.98	759.66
	(H_2ONO^+ (p))		780.87	779.38	781.86	762.11

[a] All calculations employed the 6-311++G(2df,2p) basis set and are based on the structures optimized with that basis set and the method indicated. [b] All energy values are given in kJ/mol.

$H_{298} - TS$. No scaling was applied to *ZPE* or *TE*. The final thermodynamical values for the trans-preference energy and the heterolytic bond dissociation energy are given in Table 3. Dissociation energies were computed with reference to the energies of the isolated fragment.

Several multilevel methods also were employed, and these are Gaussian-1 (G1),[23] Gaussian-2 (G2),[24] G2(MP2),[25] Gaussian-3 (G3)[26] and the Complete Basis Set-Q method (CBS-Q).[27] These multilevel approaches employ structure optimizations and vibrational frequency analysis at comparatively low levels, and these data are included in Table 1 (structures) and in the summary of the vibrational analysis (Supporting Information). The strength of the multilevel methods lies with the high level of accuracy that can often be obtained for energies using incremental adjustments for basis set improvements along with empirical corrections.

Solvent effects were determined with the isodensity surface polarized continuum model[28] (IPCM) for water ($\epsilon = 78.39$). These IPCM calculations were carried out with methods B3LYP, MPW1PW91, MP2(full), and QCISD(full) and with the basis set 6-311++G(2df,2p). In general, the IPCM calculations were based on the gas-phase structures optimized at the same theoretical level and the data thus obtained are collected in Table 4. We used the thermal data computed for the gas phase, and the approximation is well justified since solvent effects on IR spectra are minor.[29] Solvent effects on structures should be most pronounced for the electrostatic complex H_2ONO^+ and in particular on its O−N bond length. Hence, we explored the solvent effects on the structure of H_2ONO^+ using the polarized continuum model[30] (PCM) with the DFT methods, and the results of these calculations are provided as part of the Supporting Information. The effects of solvation on structures generally are minor, and even the NO bond length varies only about 0.1 Å. The structural effects of solvation cause changes in the IPCM energies that are in the millihartree range.

Calculations were carried out with Gaussian94[31] and Gaussian98[32] on an 8-processor Silicon Graphics Power Challenge L

TABLE 4: Thermodynamical Values Considering Solvation by the ICPM Model[a,b]

	methods	ΔE	ΔE_0	ΔE_{298}	ΔH_{298}	ΔG_{298}
trans-preference energy	B3LYP	4.98	4.80	4.61	4.61	4.86
	MPW1PW91	4.48	4.25	4.08	4.08	4.27
	MP2(full)	3.56	3.77	3.56	3.56	3.83
	QCISD(full)	4.35	4.39	4.18	4.18	4.40
heterolysis of neutral nitrous acid	B3LYP	287.35	271.64	275.53	278.01	241.66
	MPW1PW91	301.44	284.84	288.87	291.35	254.75
	MP2(full)	226.67	209.83	213.72	216.19	179.70
	QCISD(full)	244.11	226.98	231.00	233.48	196.95
heterolysis of protonated nitrous acid	B3LYP	25.59	17.52	18.33	20.81	−8.34
	MPW1PW91	23.22	15.30	18.36	20.84	−16.93
	MP2(full)	6.80	−0.35	−0.41	2.06	−28.76
	QCISD(full)	5.00	−2.08	−2.34	0.14	−28.01
proton affinity of nitrous acid	B3LYP			−30.67	−28.19	−49.59
	MPW1PW91			−30.44	−27.96	−56.62
	MP2(full)			15.41	17.89	−3.34
	QCISD(full)			11.45	13.93	−6.30

[a] All calculations employed the 6-311++G(2df,2p) basis set. [b] Preference energies, dissociation energies, and proton affinities in kJ/mol.

computer and on Compaq Alphaserver clusters with 8 ES40 and 8 ES45 processors.

Throughout this paper, bond lengths are given in angstroms, bond angles in degrees, total energies are in atomic units, and relative and reaction energies in kJ/mol. Experimental energies customarily are provided with a numerical accuracy of 0.01 kJ/mol, and we report the theoretical data with that numerical accuracy as well.

Results and Discussion

Available Experimental Data. *Nitrous Acid.* HONO is one of the simplest molecules to undergo cis−trans isomerization. It was reported in the 1960s that HONO suspended in N_2 matrixes at 20 K isomerizes when illuminated with infrared light and the barrier for the cis−trans isomerization is less than 50 kJ/mol.[33,34] In 1982, McDonald et al. reinvestigated the photoisomerization of HONO in solid N_2 and Ar using a tunable IR F-center laser and determined an activation barrier of 42.51 kJ/mol (3552 cm^{-1}).[35] The question as to whether the trans- or the cis-isomer of HONO is preferred received much attention. In the 1960s, McGram, et al. used IR intensity measurements and found that the trans-conformer (*E*-isomer) is more stable than the cis-conformer by 1.67 ± 0.42 kJ/mol.[36] More recently, in 1976, the microwave intensity measurements by Varma and Curl showed the same isomer preference and refined its value to $\Delta E_0^{Pref} = 1.555 \pm 0.167$ kJ/mol.[37]

Some experimental values have been reported for the homolytic bond dissociation energy of HONO. In 2000, the HO−NO bond dissociation energy of *trans*-HONO was measured using double-resonance overtone photofragment spectroscopy (DROPS) and the dissociation energy was determined to be $E_0 = 200.89$ kJ/mol (16772 ± 14 cm^{-1}).[38]

Using a crossed tunable laser−negative ion beam apparatus at a resolution of 25 μeV, the electron detachment energy of the reaction $HO^- \rightarrow HO\cdot$ was determined to be $E_0 = 176.06$ kJ/mol (14741.03 ± 0.17 cm^{-1}).[39]

The ionization energy of ·NO has been determined spectroscopically in many ways. An extrapolation of Rydberg series measured by VUV absorption spectroscopy resulted in the ionization energy of IP(NO) = 892.97 kJ/mol (9.2639 ± 0.0006 eV) and we will be using this value here.[40,41]

On the basis of these experimental data, the best experimental value for the heterolytic bond dissociation energy of HONO → $HO^- + NO^+$ is $\Delta E_0 = 917.80$ kJ/mol (Scheme 1).

SCHEME 1

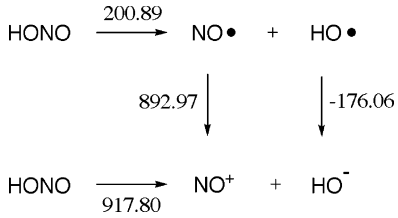

Nitrous Acidium Ion. Almost thirty years ago, Kebarle et al.[42] measured the hydration of NO^+ in the gas phase and reported a heterolytic bond dissociation energy of $\Delta H_{298} = 77.33$ kJ/mol (18.5 kcal/mol). This measurement also allowed for the determination of the proton affinity of nitrous acid and a value of $\Delta H_{298} = 784.59$ kJ/mol (187.7 kcal/mol) was derived. It appears that the structure of this important ion has never been determined experimentally.

Optimized Structures. We optimized the structures of *trans*- and *cis*-HONO and of the products of heterolysis with all methods and every basis sets and the results are documented in Table 1 of the Supporting Information and a condensed version of Table 1 with only the most pertinent data is shown. The B3LYP and MPW1PW91 calculations show little basis set effects on structures, e.g., the basis set effects on the N−O bond length in HONO are less than 0.008 Å. On the other hand, the MP2(full) and QCISD(full) structures showed more significant basis set dependency. For instance, basis set effects on the N−O bond length are as large as 0.020 Å. Figure 1 shows molecular models of the structures of the HONO isomers and of the ions HO^- and NO^+ which were calculated at the best level, CCSD(fc,T)/6-311++G(2df,2p). The latest experimental data are given for comparison in italics.[43,44] The gas-phase structure of nitrous acid has been investigated since the early fifties, the studies reveal a planar structure[45−48] and we use the data by Finnigan et al.[48] in Figure 1.

The major difference between *E*- and *Z*-HONO occurs for the N−O bond. According to the experimental values, this bond is substantially longer in the *E*-isomer (0.044 Å). On the other hand, the N=O bond in the *E*-isomer is 0.017 Å shorter than in *Z*-HONO. The N−O bond in both *E*- and *Z*-HONO is shortened and one possible explanation invokes partial double bond character due to a significant contribution by the resonance form **II**. The structures of *E*- and *Z*-HONO suggest that the polar resonance form **II** is more important in the *Z*-isomer. The calculations reproduce these trends but both the computed N−O

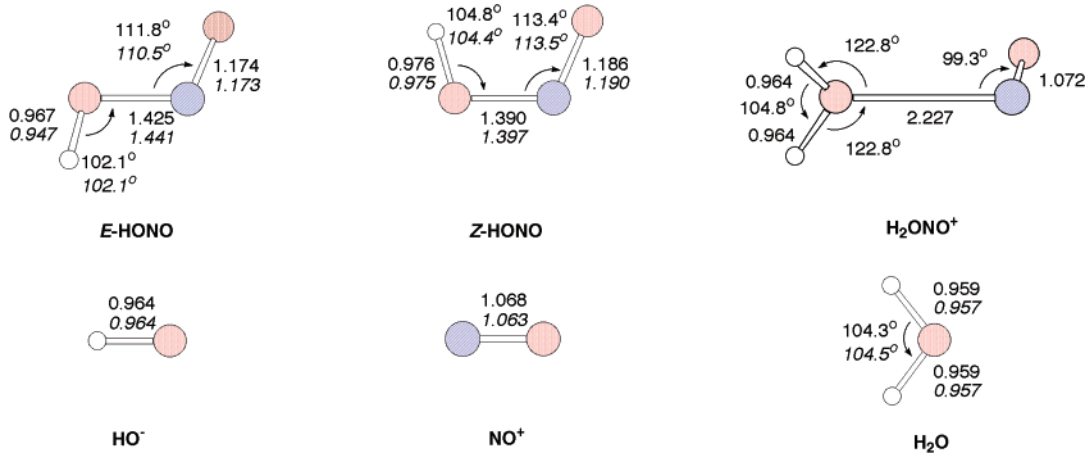

Figure 1. The CCSD(fc,T)/6-311++G(2df,2p) optimized structures of *E*- and *Z*-HONO, of protonated nitrous acid, and of the products of their O−N heterolyses. The experimental values are given in italics where available.

and N═O bonds are shorter. In particular, the computed N−O bond remains almost 0.04 Å shorter than the microwave structure.

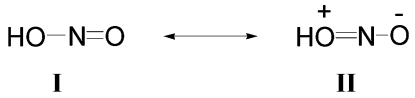

The bond in NO^+ is quite short, only 1.068 Å at the best level. Resonance form **IV** contributes and causes a bond order

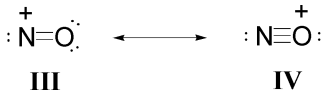

between 2 and 3. Upon addition of the hydroxide ion, the contribution of the resonance form **IV** is not only greatly diminished but it is eliminated and the polarization of this bond in HONO is in the *opposite* direction, cf. **II** of HONO. The structural discussion shows that both HONO and NO^+ enjoy resonance delocalization and this polarization is facilitated greatly with the more flexible triple-ζ valence basis sets. In Table 2 are given the isomer preference energies and dissociation energies, and these data show significant basis set effects on the energies of HONO and NO^+ in going from the "31" to the "311" basis sets.

The microwave studies suggested that the *Z*-HONO features a significantly longer H−O bond than the *E*-isomer, and this finding was interpreted as an indication for a weak intramolecular hydrogen bond.[47−49] The shorter N−O bond in *Z*-HONO

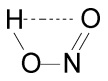

also might serve to optimize such a hydrogen-bonding interaction. But it should be recognized that the bond angles in *Z*-HONO are changed in the opposite direction; the ∠(H−O−N) and ∠(O−N−O) in *Z*-HONO are *opened* by 2.3° and 3.0°, respectively, compared to the respective angles in *E*-HONO. The calculations do not show an unusual difference in the HO bond lengths in the isomers but they do show the same trends for the angles; the ∠(H−O−N) and ∠(O−N−O) in *Z*- HONO are *opened* by 2.6° and 2.5°, respectively.

It appears that the structure of the H_2ONO^+ ion has not been determined experimentally as yet. There are however several theoretical studies of the structures of H_2ONO^+ ion[50−52] and of higher hydrate[1c−f] of NO^+ and they all show that protonation at the hydroxyl-O results in the most stable structure. This structure is C_s symmetric and the O−N═O plane is the mirror plane for the two H-atoms (Figure 1). The structure of water as one of the products of the heterolysis of the H_2ONO^+ ion also is shown in Figure 1 with experimental values in italics.[53] The structure of the H_2ONO^+ ion is that of an electrostatic complex formed between water and NO^+ cation.[54] The dative bond in H_2ONO^+ is weak and, at our highest level, leads to an unusually long N−O bond length of 2.317 Å. The calculations show an increase of the N−O bond length with improvements in the theoretical level and the basis set.

The H_2ONO^+ ion poses one noteworthy problem for the CBS-Q method which evaluates the vibrational zero-point energy at RHF/6-31G(d′). At this level the nonplanar C_s structure is a transition state while the planar C_s structure is the minimum. Entries in the tables based on the planar and non-planar structures are marked by "p" and "np", respectively. When the CBS-Q calculation is started with a nonplanar and de facto C_1 structure, then the thermochemical parameters are computed for the transition state. On the other hand, when the CBS-Q calculation is carried out with a sufficiently asymmetric initial structure that allows the RHF optimization to fall into the planar minimum, then the vibrational analysis is based on an artifact. Moreover, this artificial planar structure then causes the ion to remain planar in the following MP2(full)/6-31G(d′) optimization and all subsequent higher level energy calculations employ this wrong structure. The consequences of this problem, however, are not severe in the present case because the (imaginary) frequency of the torsion mode involved is rather low (86.5 cm^{-1} in the planar structure, 29.4 cm^{-1} in the nonplanar structure) and the planar and non-planar structures of the electrostatic complex are almost isoenergetic.

Trans-Preference Energy of HO−NO. Van Doren, et al. reported a series of computed trans-preference energies for HONO using perturbation theory as well as G1 and G2 theory.[55] It was found that the trans-conformer is more stable than the cis-conformer by 1−4 kJ/mol, depending on the level: 1.3 kJ/mol [MP2/6-31+G(d)], 4.3 kJ/mol [MP4SDTQ/6-311++G(d,p)], 1.6 kJ/mol [MP2/6-311++G(3df,3pd)], 3.4 kJ/mol (G1), and 2.5 kJ/mol (G2) and some of these data are included in Tables 1 and 3. CCSD and CCSD(T) trans-preference energies for HONO were reported by Lee and Rendell.[7] The effects of increasing the size of the basis set and/or improving the quality of the correlation treatment can be recognized best from the data presented in Table 2. At all levels, the computed trans-preference energy has the wrong sign when the basis sets

6-31G** or 6-311G** are employed. The correct sign of the trans-preference energy is reproduced only when diffuse function augmented basis sets are employed. There is hardly any difference in the trans-preference energies computed at the different levels of theory with the same basis set. With the best basis set, 6-311++G(2df,2p), trans-preferences of 2.74, 1.31, 1.73, 1.72, 2.06, 1.62, and 1.83 kJ/mol are obtained with the methods B3LYP, MPW1PW91, MP2, QCISD, QCISD(T), CCSD, and CCSD(T).

Frequency calculations were carried out at each level using the best basis set, 6-311++G(2df,2p). With the thermodynamic data we computed the E_0-, H-, and G-preferences listed in Table 3. Hence, our best computed estimate for the ΔE_0-preference is 1.83 kJ/mol which compares very well to the experimentally measured $\Delta E_0^{Pref} = 1.555 \pm 0.167$ kJ/mol.[37] Our best estimates for the enthalpy preference and the Gibbs free energy preferences are $\Delta H_{298} = 1.63$ and $\Delta G_{298} = 1.88$ kJ/mol, respectively.

The multilevel methods overestimate ΔE_0^{Pref} by 0.7−1.8 kJ/mol. Note that the Gaussian methods aim to *approximate* the QCISD(T)/6-311+G(2df,p) level, whereas our best calculations *were carried out* at the QCISD(T)/6-311++G(2df,2p) and the very similar CCSD(T)/6-311++G(2df,2p) levels. The data in Table 2 show the critical role of diffuse functions for the correct reproduction of the trans-preference energy and this same issue is manifested here again.

Heterolytic HO−NO Dissociation. Computed heterolytic bond dissociation energies ΔE^{diss}(HONO) are given in Table 2. The inclusion of diffuse functions in the basis set is essential; without diffuse functions ΔE^{diss}(HONO) is overestimated by about 150−180 kJ/mol! The obvious reason is the requirement of diffuse functions for an adequate description of the hydroxide anion formed. A second major effect is seen in going from the double-ζ to the triple-ζ valence electron description. In going from 6-31++G** to 6-311++G**, the dissociation energy drops by about 10−20 kJ/mol with any of the methods. Further improvements in the basis set cause lesser but still rather substantial changes and they generally serve to increase the dissociation energy. At the QCISD level, the dissociation energy ΔE varies moderately from 914.2, to 918.7 and to 935.3 kJ/mol as polarization is improved from 6 to 311++G(d,p) to 6-311++G(2d,p), and 6-311++G(2df,2p).

The experimental heterolytic bond dissociation energy is $\Delta E_0 = 917.80$ kJ/mol. The method dependency of the thermal corrections is minor. With the best basis set, the computed heterolytic bond dissociation energies ΔE_0 are 960.9 kJ/mol at B3LYP, 977.2 at MPW1PW91, 897.2 at MP2, 918.4 at QCISD, 928.1 at QCISD(T), 917.0 at CCSD, and 925.5 at CCSD(T). Hence, the deviations between our computation and the experimental value are 43.1 kJ/mol (B3LYP), 59.4 (MPW1PW91), −20.6 (MP2), 0.6 (QCISD), 10.3 (QCISD(T)), 0.8 (CCSD), and 7.7 kJ/mol (CCSD(T)). These data show that triple excitations have a marked effect and that the near-perfect agreement at the QCISD and CCSD levels is better than can be reasonably expected. However, in the broader perspective, *all* these higher correlated levels produce binding energies that are within 10 kJ/mol and that is excellent.

The multilevel methods perform well and G2 and G2(MP2) are particularly close to the experimental value. The G2 value of $\Delta E_0 = 918.4$ kJ/mol is within 1 kJ/mol of the experimental value. These outcomes are encouraging in that the Gaussian and CBS-Q methods require much less computer time (more than a magnitude). On the other hand, one also has to realize that the accuracies of the G2 and G2(MP2) dissociation energies ostensibly are better than the accuracies of the calculations of any of the molecules involved in the dissociation.

Density functional theory frequently is considered to be more reliable than the traditional correlation methods. For example, a recent systematic study of dissociation energies of halogenated molecules shows various density functional methods to outperform QCISD(T) and CCSD(T) methods and average deviations for the DFT-derived dissociation energies are less than 15 kJ/mol.[56] Several studies suggested that DFT presents a reliable method for the computation of bond dissociation energies.[57] Our case study shows a disappointing performance of the DFT methods while the performances of the traditional correlation methods meet expectations. It remains to be seen whether this failure of DFT is a general problem for heterolyses. The HO−NO heterolysis clearly is a particularly challenging problem because the bond cleavage is accompanied by major electronic relaxation in both fragments (vide infra).

Our best estimates for the reaction enthalpy and the reaction Gibbs free energy of the HO−NO heterolysis are $\Delta H_{298} = 931.8$ and $\Delta G_{298} = 895.5$ kJ/mol, respectively.

Nitrous Acidium Ion Heterolysis. The experimental proton affinity of 784.6 kJ/mol is reasonably well reproduced at all levels of theory so long as good basis sets are employed (Table 3). Perturbation and configuration interaction theory result in proton affinities that are overestimated while the DFT results are underestimated by roughly the same amount. Remarkably, the multilevel methods G2, G2(MP2), G3, and CBS-Q give near-perfect proton affinities.

The heterolytic dissociation energy $\Delta H_{298} = 77.3$ kJ/mol is matched closely by the computations with the best basis set; ΔH_{298}(MP2) = 82.4 kJ/mol, ΔH_{298}(QCISD) = 79.7 kJ/mol, ΔH_{298}(QCISD(T)) = 82.1 kJ/mol, ΔH_{298}(CCSD) = 79.0 kJ/mol, and ΔH_{298}(CCSD(T)) = 81.6 kJ/mol. Francisco recently reported[52] binding energies of $\Delta E = 78.2$ and 77.3 kJ/mol at the QCISD(T)/6-311++G(2df,2p) and QCISD(T)/6-311++G(3df,3pd) levels. This paper made no reference to the experimental work, and no thermal analysis was carried out. Our work shows (Table 3) the best prediction for the dissociation energy based on the CCSD(fc,T) data is 81.6 kJ/mol. All of these data—MP2, QCISD, and CCSD—are within 5 kJ/mol of the experimental value. The multilevel methods G2, G2(MP2), and G3 all accomplish similar accuracies while G1 and CBS-Q overestimate by 7−9 kJ/mol.

Heterolytic dissociation energies of $\Delta H_{298} = 107.3$ kJ/mol and $\Delta H_{298} = 107.0$ kJ/mol are predicted by B3LYP and MPW1PW91 in conjunction with the 6-311++G(2df,2p) basis set. These values overestimate the bond strength by about 30 kJ/mol; an error of almost 50%. The source of this error is hard to trace. For neutral HONO, the electronic relaxations upon bond cleavage are dramatic (anion formation, changes in bond polarities, etc.) and large correlation effects are to be expected. The dissociation of the electrostatic complex, however, leaves the structures of the fragments almost the same and the electronic relaxations also are much less as compared to the HONO dissociation.

Effects of Aqueous Solvation. The computation of solvation effects remains challenging and requires the use of approximative theory. Here, we employed the isodensity surface polarized continuum model (IPCM) to determine the solvation energies[28] for aqueous solution, and the results are summarized in Table 4. The calculations consistently show at all levels that the trans-preference of nitrous acid persists and increases in aqueous solution. Our discussion focuses on the heterolyses of neutral and protonated HONO and on the proton affinity of HONO.

The heterolysis of neutral HONO generates two ions and this heterolytic dissociation energy is lowered by about 700 kJ/mol but it remains nevertheless on the order of 200 kJ/mol. The heterolysis of protonated nitrous acid to water and a smaller cation also benefits from solvation, but the solvent effect of about 80 kJ/mol on the dissociation energy is a magnitude lower compared to the HONO dissociation. In this case, however, the solvation has a qualitative effect because it renders the heterolysis almost thermoneutral and ΔG_{298} even becomes negative. Hence, polar solution can reduce the intrinsically already low stability of the electrostatic complex between water and NO^+ even more. The calculations thus suggest that the protonation of nitrous acid can be seen as generating essentially free NO^+ cations in aqueous solution.

The enthalpy of hydration $\Delta H_{298}(H^+) = -262.2$ kcal/mol and the Gibbs free energy of hydration $\Delta G_{298}(H^+) = -262.5$ kcal/mol (gas phase to water transfer) were taken from the literature.[58] The inclusion of solvation reduces the proton affinity of HONO to almost nothing and, in fact, at the best levels the proton affinity ΔG_{298} becomes even slightly negative. This result suggests a qualitative difference in the mechanisms of NO^+ formation in the gas-phase and in solution. In the gas-phase, the protonation of HONO is fast and the heterolysis of the nitrous acidium ion determines NO^+ concentrations. Note that the gas-phase proton affinity of water is 696.8 kJ/mol[59] and proton transfer from hydronium ion to HONO in the gas phase thus also is highly exothermic. In solution, however, the protonation of HONO is the rate-limiting step and, once protonation occurs, it leads directly to the formation of an essentially free NO^+ cation in aqueous media. While the gas-phase proton affinities show the protonation of HONO to be a greatly exothermic process, this does not seem to be the case in solution because such a proton transfer would replace the well-solvated hydronium ion by the much less well-solvated nitrous acidium ion.

Conclusion

On the basis of reported measurement of the homolytic HO−NO bond dissociation energy, the electron affinity of HO, and the ionization energy of NO, we determined the best experimental value for the heterolytic bond dissociation energy of $HO-NO \rightarrow HO^- + NO^+$ and it is $\Delta E_0 = 917.8$ kJ/mol. With the best basis set 6-311++G(2df,2p) employed in the present study, the computed heterolytic bond dissociation energies ΔE_0 are 897.2 kJ/mol at MP2, 918.4 at QCISD, 928.1 at QCISD(T), 917.0 at CCSD, and 925.5 kJ/mol at CCSD(T). For H_2ONO^+ the experimental heterolytic bond dissociation energy is $\Delta H_{298} = 77.3$ kJ/mol and, again with the best basis set 6-311++G(2df,2p), the computed ΔH_{298} values are 82.4 kJ/mol at MP2, 79.7 at QCISD, 82.1 at QCISD(T), 79.0 at CCSD, and 81.6 kJ/mol at CCSD(T).

Among the multilevel methods, the best results consistently were obtained at the G2 level; $\Delta E_0^{diss}(HO-NO) = 918.4$ kJ/mol and $\Delta H_{298}^{diss}(H_2O^+-NO) = 81.4$ kJ/mol. The computationally more efficient G2-mimics G2(MP2) and G3 also gave results in close agreement with the G2 data.

The deviations between the DFT computations and the experimental value are much larger than for the traditional correlation methods. With the best basis set 6-311++G(2df,2p), the computed heterolytic bond dissociation energies ΔE_0 of HO−NO are 960.9 at 977.2 kJ/mol at B3LYP and MPW1PW91, and for H_2ONO^+ the heterolytic bond dissociation energies ΔH_{298} are 107.3 and 107.0 at B3LYP and MPW1PW91. It remains to be seen whether this failure of DFT is a general problem for heterolyses. The HO−NO heterolysis is a particularly challenging problem because bond cleavage is accompanied by major electronic relaxation in both fragments and, in fact, it was this recognition that caused us to carry out the study presented here.

Despite a large solvent catalysis, the calculations suggest that the heterolysis of neutral HONO still would require about 200 kJ/mol and this reaction channel thus is unlikely at room and physiological temperatures. As to the proton-catalyzed process, our study suggests different mechanisms for NO^+ formation in gas-phase (fast protonation, slow heterolysis) and in solution (slow protonation, spontaneous heterolysis).

Acknowledgment. This work was supported by grants from the National Cancer Institute (R01CA85538) and the National Institutes of Health of the United States (GM61027). We thank IATS for generous allocations of computer time on the MU Research Computing Facilities and Drs. Gordon Springer and Larry Sanders for their assistance.

Supporting Information Available: Supporting Information Available: Two tables that contain the structures of *E*- and *Z*-HONO, of H_2ONO^+, and of the products of their heterolyses at all levels considered, an extended version of Table 2 that includes the total energies of *E*- and *Z*-HONO, HO^-, NO^+, H_2O, and H_2ONO^+, and a table of G1, G2, G2(MP2), G3, and CBS-Q energies, a table listing the computed thermodynamical parameters, and three tables with the results of IPCM and PCM studies of structural effects of solvation. This material is available free of charge via the Internet at http://pubs.acs.org.

References and Notes

(1) (a) Kirchstetter, T. W.; Harley, R. A. *Environ. Sci. Technol*. **1996**, *30*, 2843. (b) Chou, A.; Li, Z.; Tao, F. M. *J. Phys. Chem. A* **1999**, *103*, 7848. (c) Reynolds, C. A.; Thomson, C. *Int. J. Quantum Chem: Quantum Bio. Symp.* **1986**, *12*, 263. (d) Hamman, E.; Lee, E. P. F.; Dyke, J. M. *J. Phys. Chem. A* **2001**, *105*, 5528. (e) Wainman, T.; Weschler, C. J.; Lioy, P. J.; Zhang, J. *Environ. Sci. Technol.* **2001**, *35*, 2200. (f) Heland, J.; Kleffmann, J.; Kurtenbach, R.; Wiesen, P. *Environ. Sci. Technol.* **2001**, *35*, 3207.

(2) Tsang, W.; Herron, J. T. *J. Phys. Chem. Ref. Data* **1991**, *20*, 609.

(3) Smith, M. B.; March, J. *Advanced Organic Chemistry, Reaction Mechanisms, and Structure*, 5th ed.; Wiley: New York, 2001.

(4) (a) Tamir, S.; Burney, S.; Tannenbaum, S. R. *Chem. Res. Toxicol.* **1996**, *9*, 821. (b) Adams, J. B. *Food. Chem.* **1997**, *59*, 401. (c) Oldreive, C.; Zhao, K.; Paganga, G.; Halliwell, B.; Rice-Evans, C. *Chem. Res. Toxicol.* **1998**, *11*, 1574. (d) O'Donnell, V. B.; Eiserich, J. P.; Chumley, P. H.; Jablonsky, M. J.; Krishna, N. R.; Kirk, M.; Barnes, S.; Darley-Usmar, V. M.; Freeman, B. A. *Chem. Res. Toxicol.* **1999**, *12*, 83.

(5) (a) Smith, P. S.; Loeppky, R. N. *J. Am Chem. Soc*. **1967**, *89*, 1147. (b) Loeppky, R. N. In *Nitrosamines and Related N-Nitroso Compounds—Chemistry and Biochemistry;* Loeppky, R. N., Michejda, C. J., Eds.; Am. Chem. Soc.: Washington, D C, 1994; pp 1−18, 52−65. (c) Loeppky, R. N.; Singh, S. P.; Elomari, S.; Hastings, R.; Theiss, T. E. *J. Am. Chem. Soc.* **1998**, *120*, 5193. (d) Loeppky, R. N.; Elomari, S. *J. Org. Chem.* **2000**, *65*, 96.

(6) Loeppky, R. N.; Fuchs, A.; Janzowski, C.; Goelzer, P.; Scheider, H.; Eisenbrand, G. *Chem. Res. Toxicol.* **1998**, *11*, 1556. (b) Loeppky, R. N.; Goelzer, P. *Chem. Res. Toxicol.* **2002**, *15*, 457. (c) Loeppky, R. N.; Ye, Q.; Goelzer, P.; Chen, Y. *Chem. Res. Toxicol.* **2002**, *15*, 470.

(7) Lee, T. J.; Rebdell, A. P. *J. Chem. Phys.* **1991**, *94*, 6229.

(8) (a) Hohenberg, P.; Kohn, W. *Phys. Rev. B* **1964**, *136*, 864. (b) Kohn, W.; Sham, L. J. *Phys. Rev. A* **1965**, *140*, 1133. (c) Pople, J. A.; Gill, P. M. W.; Johnson, B. G. *Chem. Phys. Lett*. **1992**, *199*, 557. (d) Johnson, B. G.; Frisch, M. J. *Chem. Phys. Lett*. **1993**, *216*, 133. (e) Johnson, B. G.; Frisch, M. J. *J. Chem. Phys*. **1994**, *100*, 7429. (d) Stratmann, R. E.; Burant, J. C.; Scuseria, G. E.; Frisch, M. J. *J. Chem. Phys*. **1997**, *106*, 10175.

(9) (a) Head-Gordon, M.; Pople, J. A.; Frisch, M. J. *Chem. Phys. Lett*. **1988**, *153*, 503. (b) Frisch, M. J.; Head-Gordon, M.; Pople, J. A. *Chem. Phys. Lett*. **1990**, *166*, 275, 281. (c) Head-Gordon, M.; Head-Gordon, T. *Chem. Phys. Lett*. **1994**, *220*, 122.

(10) Pople, J. A.; Head-Gordon, M.; Raghavachari, K. *J. Chem. Phys*. **1987**, *87*, 5968.

(11) (a) Purvis, G. D., III.; Bartlett, R. J. *J. Chem. Phys.* **1982**, *76*, 1910. (b) Scuseria, G. E.; Schaefer, H. F. *J. Chem. Phys.* **1989**, *90*, 3700.

(12) Becke, A. D. *J. Chem. Phys.* **1993**, *98*, 5648.

(13) (a) Lee, C.; Yang, W.; Parr, R. G. *Phys. Rev. B* **1988**, *37*, 785. (b) Miehlich, B.; Savin, A.; Stoll, H.; Preuss, H. *Chem. Phys. Lett.* **1989**, *157*, 200.

(14) (a) Becke, A. D. *J. Chem. Phys.* **1993**, *98*, 5648. (b) Hohenberg, P.; Kohn, W. *Phys. Rev. B* **1964**, *136*, 864. (c) Kohn, W.; Sham, L. J. *Phys. Rev. A* **1965**, *140*, 1133.

(15) (a) Raghavachari, K. *Theor. Chem. Acc.* **2000**, *103*, 361. (b) Curtiss, L. A.; Raghavachari, K.; Redfern, P. C.; Pople, J. A. *J. Chem. Phys.* **1997**, *106*, 1063. (c) Clark, D. L.; Hobart, D. E.; Neu, M. P. *Chem. Rev.* **1995**, *95*, 25.

(16) Adamo, C.; Barone, V. *J. Chem. Phys.* **1998**, *108*, 664.

(17) (a) Burke, K.; Perdew, J. P.; Wang, Y. Derivation of a generalized gradient approximation: The PW91 density functional. In *Electronic Density Functional Theory: Recent Progress and New Directions*; Dobson, J. F., Vignale, G., Das, M. P., Eds.; Plenum: New York, 1998; p 81. (b) Perdew, J. P. In *Electronic Structure of Solids*' 91; Ziesche, P., Eschrig, H., Eds.; kademie Verlag: Berlin, 1991; 11.

(18) (a) Perdew, J. P.; Chevary, J. A.; Vosko, S. H.; Jackson, K. A.; Perderson, M. R.; Singh, D. J.; Fiolhais, C. *Phys. Rev. B* **1992**, *46*, 6671. (b) Perdew, J. P.; Chevary, J. A.; Vosko, S. H.; Jackson, K. A.; Perderson, M. R.; Singh, D. J.; Fiolhais, C. *Phys. Rev. B* **1993**, *48*, 4978. (c) Perdew, J. P.; Burke, K.; Wang, Y. *Phys. Rev. B* **1996**, *54*, 16533.

(19) 31G* and 6-31G**: (a) Pople, J.; Beveridge, D.; Dobosh, P. *J. Am. Chem. Soc.* **1968**, *90*, 4201. (b) Hariharan, P. C.; Pople, J. A. *Theor. Chim. Acta* **1973**, *28*, 213. (C) Hariharan, P. C.; Pople, J. A. *Chem. Phys. Lett.* **1977**, *51*, 192. (c) second-row: Francl, M. M.; Pietro, W. J.; Hehre, W. J.; Binkley, J. S.; Gordon, M. S.; DeFrees, D. J.; Pople, J. A. *J. Chem. Phys.* **1982**, *77*, 3654.

(20) 311G: (a) Krisnan, R.; Binkley, J. S.; Seeger, R.; Pople, J. A. *J. Chem. Phys.* **1980**, *72*, 650. (b) Krisnan, R.; Frisch, M. J.; Pople, J. A. *J. Chem. Phys.* **1980**, *72*, 4244.

(21) Diffuse functions: Clark, T.; Chandrasekhar, J.; Spitznagel, G. W.; Schleyer, P. v. R. *J. Comput. Chem.* **1983**, *4*, 294.

(22) Multiple polarization functions: (a) Binkley, J. S.; Pople, J. A. *Int. J. Quantum Chem.* **1975**, *9*, 229. (b) Frisch, M. J.; Pople, J. A.; Binkley, J. S. *J. Chem. Phys.* **1984**, *80*, 3265.

(23) (a) Pople, J. A.; Head-Gordon, M.; Fox, D. J.; Raghavachari, K.; Curtiss, L. A. *J. Chem. Phys.* **1989**, *90*, 5622. (b) Curtiss, L. A.; Jones, C.; Trucks, G. W.; Raghavachari, K.; Pople, J. A. *J. Chem. Phys.* **1990**, *93*, 2537.

(24) Curtiss, L. A.; Raghavachari, K.; Trucks, G. W.; Pople, J. A. *J. Chem. Phys.* **1991**, *94*, 7221.

(25) Curtiss, L. A.; Raghavachari, K.; Pople, J. A. *J. Chem. Phys.* **1993**, *98*, 1293.

(26) Curtiss, L. A.; Raghavachari, K.; Redfern, P. C.; Rassolov, V.; Pople, J. A. *J. Chem. Phys.* **1998**, *109*, 7764.

(27) Ochterski, J. W.; Petersson, G. A.; Montgomery, J. A., Jr. *J. Chem. Phys.* **1996**, *104*, 2598.

(28) Foresman, J. B.; Keith, T. A.; Wiberg, K. B.; Snoonian, J.; Frisch, M. J. *J. Phys. Chem.* **1996**, *100*, 16098.

(29) Reichardt, C. *Solvents and Solvent Effects in Organic Chemistry*, 2nd ed.; VCH: Weinheim, 1988; Chapter 6.

(30) (a) Miertus, S.; Scrocco, E.; Tomasi, J. *Chem. Phys.* **1981**, *55*, 117. (b) Cossi, M.; Barone, V.; Cammi, R.; Tomasi, J. *Chem. Phys. Lett.* **1996**, *255*, 327. (c) Barone, V.; Cossi, M.; Mennucci, B.; Tomasi, J. *J. Chem. Phys.* **1997**, *107*, 3210. (d) Barone, V.; Cossi, M. *J. Phys. Chem. A* **1998**, *102*, 1995.

(31) Frisch, M. J.; Trucks, G. W.; Schlegel, H. B.; Gill, P. M. W.; Johnson, B. G.; Robb, M. A.; Cheeseman, J. R.; Keith, T.; Petersson, G. A.; Montgomery, J. A.; Raghavachari, K.; Al-Laham, M. A.; Zakrzewski, V. G.; Ortiz, J. V.; Foresman, J. B.; Cioslowski, J.; Stefanov, B. B.; Nanayakkara, A.; Challacombe, M.; Peng, C. Y.; Ayala, P. Y.; Chen, W.; Wong, M. W.; Andres, J. L.; Replogle, E. S.; Gomperts, R.; Martin, R. L.; Fox, D. J.; Binkley, J. S.; Defrees, D. J.; Baker, J.; Stewart, J. P.; Head-Gordon, M.; Gonzalez, C.; Pople, J. A. *Gaussian 94*, Revision C.3; Gaussian Inc.: Pittsburgh, PA, 1995.

(32) Frisch, M. J.; Trucks, G. W.; Schlegel, H. B.; Scuseria, G. E.; Robb, M. A.; Cheeseman, J. R.; Zakrzewski, V. G.; Montgomery, J. A.; Stratmann, Jr. R. E.; Burant, J. C.; Dapprich, S.; Millam, J. M.; Daniels, A. D.; Kudin, K. N.; Strain, M. C.; Farkas, O.; Tomasi, J.; Barone, V.; Cossi, M.; Cammi, R.; Mennucci, B.; Pomelli, C.; Adamo, C.; Clifford, S.; Ochterski, J.; Petersson, G. A.; Ayala, P. Y.; Cui, Q.; Morokuma, K.; Malick, D. K.; Rabuck, A. D.; Raghavachari, K.; Foresman, J. B.; Cioslowski, J.; Ortiz, J. V.; Baboul, A. G.; Stefanov, B. B.; Liu, G.; Liashenko, A.; Piskorz, P.; Komaromi, I.; Gomperts, R.; Martin, R. L.; Fox, D. J.; Keith, T.; Al-Laham, M. A.; Peng, C. Y.; Nanayakkara, A.; Challacombe, M.; Gill, P. M. W.; Johnson, B.; Chen, W.; Wong, M. W.; Andres, J. L.; Gonzalez, C.; Head-Gordon, M.; Replogle, E. S.; Pople, J. A. *Gaussian 98*; Gaussian, Inc.: Pittsburgh, PA, 1998.

(33) Hall, R. T.; Pimentel, G. C. *J. Chem. Phys.* **1963**, *38*, 1889.

(34) Baldeschwieler, J. D.; Pimentel, G. C. *J. Chem. Phys.* **1960**, *30*, 108.

(35) McDonald, P. A.; Shirk, J. S. *J. Chem. Phys.* **1982**, *77*, 2355.

(36) McGraw, G. E.; Bernitt, D. L.; Hisatsune, I. C. *J. Chem. Phys.* **1966**, *45*, 1392.

(37) Varma, R.; Curl, R. F. *J. Phys. Chem.* **1976**, *80*, 402.

(38) Reiche, F.; Abel, B. *J. Chem. Phys.* **2000**, *112*, 8885.

(39) Schulz, P. A.; Mead, R. D.; Jones, P. L.; Lineberger, W. C. *J. Chem. Phys.* **1982**, *77*, 1153.

(40) Miescher, E. *Can. J. Phys.* **1976**, *54*, 2074.

(41) (a) Reiser, G.; Habenicht, W.; Schlag, E. W. *Chem. Phys. Lett.* **1988**, *152*, 119. (b) We are aware that, Schlag, et al. more recently, in 1988, determined the ionization energy of nitric oxide using zero kinetic energy photoelectron spectroscopy (ZEKE PES) and obtained a value of IP(NO) = 894.98 kJ/mol (74719.0 cm^{-1}). Note that Schlag et al. commented that "the most accurate method is extrapolation of Rydberg series but rarely applicable in practice, since, for example, the rotational structure must be fully resolved. This can be done only for a very few molecules. ZEKE PES is a tool that can be applied without any such restrictions with equivalent accuracy."

(42) French, M. A.; Hills, L. P.; Kebarle, P. *Can. J. Chem.* **1973**, *51*, 456.

(43) NO^+: Laane, J.; Ohlsen, J. R. *Prog. Inorg. Chem.* **1980**, *27*, 465.

(44) HO^-: (a) Owrutsky, J. C.; Rosenbaum, N. H.; Tack, L. M.; Saykally, R. J. *J. Chem. Phys.* **1985**, *83*, 5338. (b) Rosenbaum, N. H.; Owrutsky, J. C.; Tack, L. M.; Saykally, R. J. *J. Chem. Phys.* **1986**, *84*, 5308.

(45) Jones, L. H.; Badger, R. M.; Moore, G. E. *J. Chem. Phys.* **1951**, *19*, 1599.

(46) Cox, A. P.; Kuczkowski, R. L. *J. Am. Chem. Soc.* **1966**, *88*, 5071.

(47) Finnigan, D. J.; Cox, A. P.; Brittain, A. H.; Smith, J. G. *J. Chem. Soc., Faraday Trans.* **1972**, *68*, 548.

(48) Cox, A. P.; Ellis, M. C.; Attfield, C. J.; Ferris, A. C. *J. Mol. Struct.* **1994**, *320*, 91.

(49) Cox, A. P.; Brittain, A. H.; Finnigan, D. J. *Faraday Trans. Soc.* **1971**, *67*, 2179.

(50) Nguyen, M.; Hegarty, A. F. *J. Chem. Soc., Perkin. Trans. 2* **1984**, 2037.

(51) Petris, G. D.; Marzio, A. D.; Grandinetti, F. *J. Phys. Chem.* **1991**, *95*, 9782.

(52) Francisco, J. S. *J. Chem. Phys.* **2001**, *115*, 2117.

(53) Hasted, J. B. In *Water, A comprehensive treatise*; Franks, F., Ed.; Plenum Press: New York, 1972; *1*, 255.

(54) For electrostatic complexes, see: Glaser, R.; Farmer, D. *Chem. Eur. J.* **1997**, *3*, 1244 and references therein.

(55) Van Doren, J. M.; Viggiano, A. A.; Morris, R. A.; Stevens Miller, A. E.; Miller, T. M.; Paulson, J. F. *J. Chem. Phys.* **1993**, *98*, 7948.

(56) Lazarou, Y. G.; Prosmitis, A. V.; Papadimitriou, V. C.; Papagiannakopoulus, P. *J. Phys. Chem. A* **2001**, *105*, 6729.

(57) (a) Jursic, B. S. *J. Mol. Struct. (THEOCHEM)* **1996**, *366*, 103. (b) Jursic, B. S. *J. Mol. Struct. (THEOCHEM)* **1996**, *370*, 65. (c) Jursic, B. S. *J. Mol. Struct. (THEOCHEM)* **1998**, *422*, 253. (d) Wiener, J. M.; Politzer, P. *J. Mol. Struct. (THEOCHEM)* **1998**, *427*, 171. (e) Jursic, B. S. *J. Chem. Soc., Perkin Trans.* **1999**, *2*, 369. (f) Jursic, B. S. *Chem. Phys. Lett.* **1999**, *299*, 334. (g) Jursic, B. S. *J. Mol. Struct. (THEOCHEM)* **1999**, *459*, 23. (h) Jursic, B. S. *J. Mol. Struct. (THEOCHEM)* **1999**, *467*, 173.

(58) Lim, C.; Bashford, D.; Karplus, M. *J. Phys. Chem.* **1991**, *95*, 5610.

(59) Collyer, S. M.; McMahon, T. B. *J. Phys. Chem.* **1983**, *87*, 909.